Supplementary Information for

Iron colloids dominate sedimentary supply to the ocean interior

William B Homoky[ab1], Tim M Conway[c], Seth G John[d], Daniela König[e], FeiFei Deng[b], Alessandro Tagliabue[e], Rachel A. Mills[f]

[a]University of Leeds, School of Earth and Environment, UK
[b]University of Oxford, Department of Earth Sciences, UK
[c]University of South Florida, College of Marine Science, USA
[d]University of Southern California, Department of Earth Sciences, USA
[e]University of Liverpool, School of Environmental Sciences, UK
[f]University of Southampton, School of Ocean and Earth Science, UK

[1] To whom correspondence should be addressed. Email: W.Homoky@leeds.ac.uk

Supplementary Information text

SI Text 1. Equations of Fe isotope fractionation and mass balance. Two experimental scenarios are used to simulate the controls of dFe isotope composition in porewater from GA10W Station 21. In each scenario, the isotope composition of soluble Fe ($\delta^{56}sFe$) is described by a Rayleigh fractionation equation:

$$\delta^{56}sFe = \left(\delta^{56}sFe_0 + 10^3\right) * \left(\frac{[sFe]}{[sFe_0]}\right)^{\alpha-1} - 10^3 \qquad \text{[Eq. S1]}$$

Where the deepest sample (8.5 cmbsf, from the top of the ferruginous zone) defines the initial soluble Fe concentration ($[sFe_0]$) and soluble Fe isotope composition ($\delta^{56}sFe_0$) entering the oxic-nitrogenous zone and two variants of the fraction factor (α) were set as follows:

In scenario 1, colloidal Fe is assumed to be Fe_{IOH} (though it could represent other authigenic sinks) produced from soluble Fe that is assumed to be $Fe(II)_{aq}$. Thus $\delta^{56}cFe$ reflects the fractionation effect (α) associated with $Fe(II)_{aq}$ oxidation and precipitation to Fe_{IOH}:

$$\delta^{56}cFe = \delta^{56}sFe + (\alpha - 1) * 10^3. \qquad \text{[Eq. S2]}$$

In scenario 2, colloidal Fe is assumed to be derived entirely from lithogenic material without a fractionation effect and a crustal Fe isotope composition of 0.08‰ is prescribed based on the average composition measured in South Atlantic margin sediments from GA10E (1). At any depth interval, the isotope composition of dFe is predicted using the isotope mass-balance equation,

$$\delta^{56}dFe = \frac{[sFe]}{[dFe]} * \delta^{56}sFe + \frac{[cFe]}{[dFe]} * \delta^{56}cFe, \qquad \text{[Eq. S3]}$$

where predicted $\delta^{56}dFe$ is equal to the sum of the product of the soluble Fe fraction ($[sFe]/[dFe]$) and its isotope composition ($\delta^{56}sFe$, Eq. S1) and the product of the colloidal Fe fraction ($[cFe]/[dFe]$) and its isotope composition ($\delta^{56}cFe$, Eq. S2).

Initial values of $\delta^{56}sFe_0$ set in Equation S1 were chosen so that $\delta^{56}dFe$, calculated from Equation S3, matched the measured initial isotope composition of dFe at the lower boundary of 8.5 cmbsf. A summary of the parameterizations used in model experiments is as follows:

Scenario 1a: $\delta^{56}sFe_0$ = -1.02‰, α = 1.0005, $\delta^{56}cFe$ = Eq. S2

Scenario 1b: $\delta^{56}sFe_0$ = -0.62‰, α = 0.9995, $\delta^{56}cFe$ = Eq. S2

Scenario 2a: $\delta^{56}sFe_0$ = -1.46‰, α = 1.0005, $\delta^{56}cFe$ = 0.08‰

Scenario 2b: $\delta^{56}sFe_0$ = -1.46‰, α = 0.9995, $\delta^{56}cFe$ = 0.08‰

SI Text 2. Variants of α. A two-step reaction model (Eq. S4) has previously been used to explain Fe isotope fractionations observed in modern aqueous environments (*2, 3*).

$$\textbf{Fe(II)}_{aq} \overset{k_1}{\leftrightarrow} \textbf{Fe(III)}_{aq} \overset{k_2}{\rightarrow} \textbf{Fe}_{IOH} \qquad\qquad \text{[Eq. S4]}$$

In most natural environments and experiments the reaction rate constant of $Fe(II)_{aq}$ oxidation to $Fe(III)_{aq}$ (k_1) is smaller than the rate constant for $Fe(III)_{aq}$ precipitation as insoluble oxides ($k_2 > k_1$); Isotopic exchange is sufficiently rapid between aqueous Fe(II) and Fe(III) – faster than the rate of $Fe(II)_{aq}$ oxidation to $Fe(III)_{aq}$ (k_1) – that they maintain isotopic equilibrium, such that $Fe(II)_{aq}$ oxidation and precipitation to Fe_{IOH} can be described by an overall isotopic equilibrium-dominated fractionation factor $\Delta^{56}Fe_{IOH-Fe(II)} > 0‰$ or $\alpha\,^{56}Fe_{IOH-Fe(II)} > 1$. Such α values are used to explain the behavior of Fe isotopes in many aqueous environments, such as continental streams (*4*) and groundwater (*5*), ocean hydrothermal plumes (*6*) and deposits (*7*). However, oxidation fronts in anoxic ocean basins with steep concentration gradients in $Fe(II)_{aq}$, which could be analogous to oxidation fronts in porewater, have also indicated that the rate constant k_1 could exceed k_2 and prevent aqueous Fe species from reaching isotopic equilibrium to an extent that produces a kinetics-dominated reversal in the overall isotope fractionation effect between $Fe(II)_{aq}$ and Fe_{IOH} (i.e. $\Delta^{56}Fe_{IOH-Fe(II)} < 0‰$ or $\alpha\,^{56}Fe_{IOH-Fe(II)} < 1$; (*8, 9*)). Staubwasser *et al.* (*9*) explores these arguments in some detail based on dFe isotopes in a redox stratified water-column. It has since also been a preferred explanation for hints of heavier dFe isotope enrichment found in pore waters near oxidising fronts in some fjord sediments (*10*). Homoky *et al.* (*1*) did not consider the potential significance of such a reversal in isotope fractionation during their interpretation of pore water dFe isotopes in from the Cape margin sediments of GA10E. For completeness therefore, we have duplicated the isotope mass-balance scenarios described herein with values of $\alpha < 1$ and > 1 (0.9995 and 1.0005) during soluble Fe oxidation.
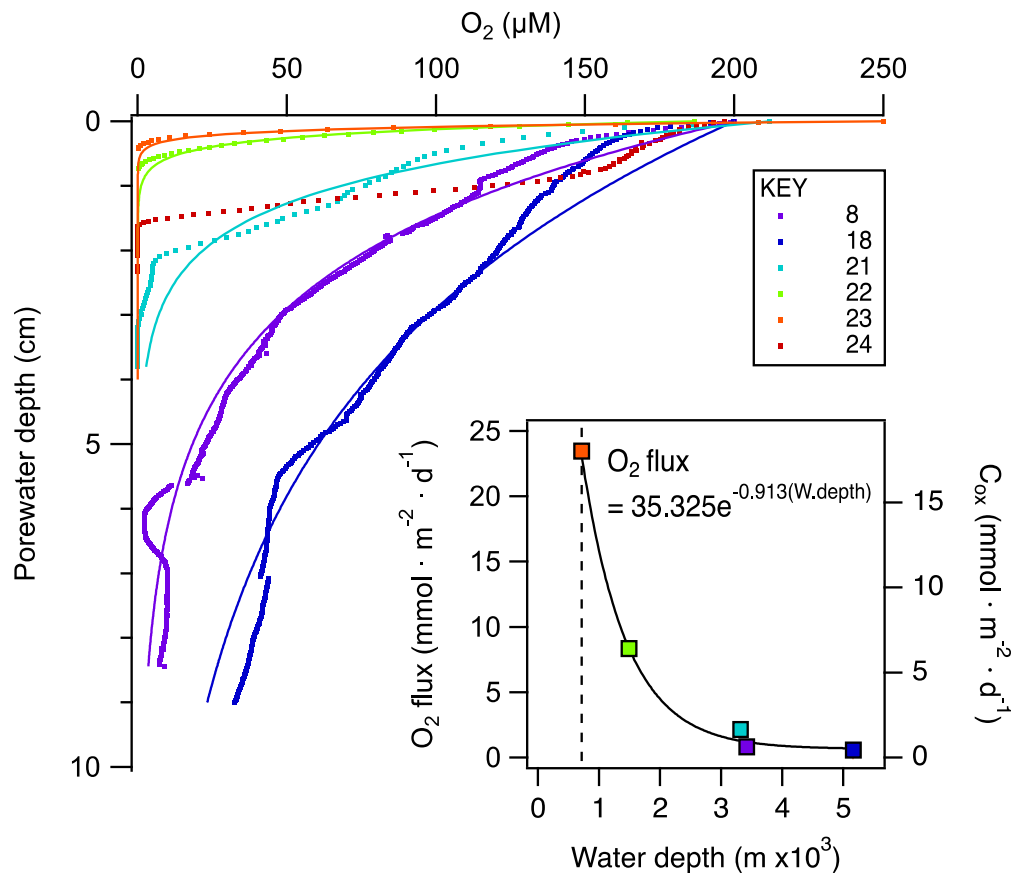
Figure S1. Porewater O₂ depth profiles and calculated O₂ consumption rates. Discrete observations are shown by individual data markers. 1-D steady-state consumption model fits to these data are indicated by solid lines, and are used to calculate deep-water O₂ consumption and organic C oxidation rates presented by the inset following the approach of Klar *et al.* (*11*) and the original work of Berner (*12*). The permeable nature of shallow sandy sediments at station 24, precluded this site from our flux assessment.
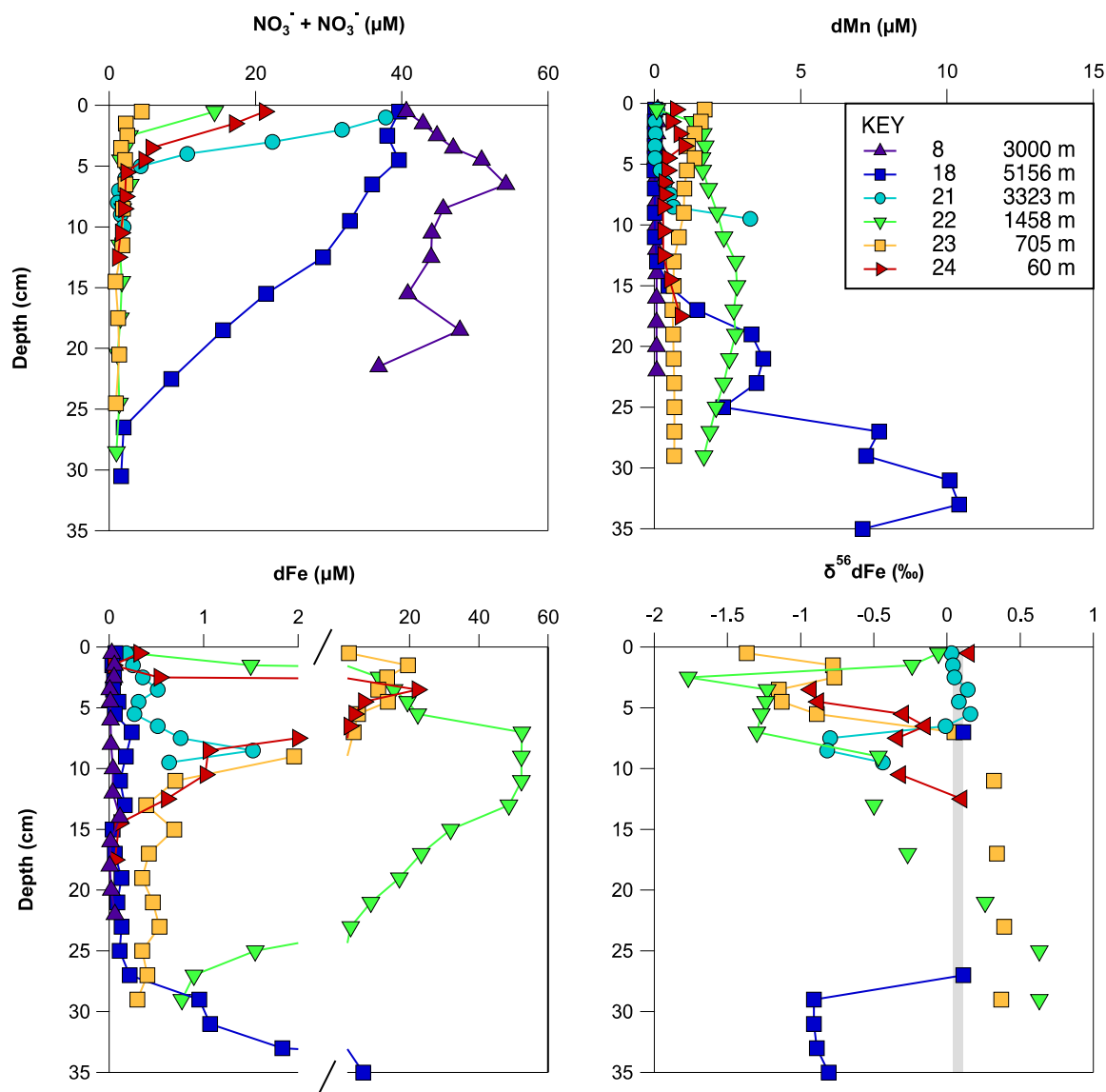
Figure S2. Porewater NO₃⁻ + NO₃⁻, dMn, dFe and δ⁵⁶Fe depth profiles from GA10W. Error bars (±2sigma) are within the size of individual data markers. Porewater maxima in dMn and dFe concentration underlie surface maxima in nitrous oxides at all sites, except for St 8 (Mid-Atlantic Ridge) where no dMn or dFe maxima were identified. Porewater δ^{56}Fe values in surface nitrogenous zones are similar to the composition of crustal rocks (grey bar). Porewater δ^{56}Fe values are lighter than the composition of crustal rocks in underlying zones of dFe maxima. Porewater δ^{56}Fe values reach values heavier than the composition of crustal rocks in zones underlying dFe maxima.

Table S1. GA10W Sediment sampling stations and physical properties

Station	Latitude deg. N	Longitude deg. E	Water depth m	Sed. depth range cm	DBD g · cm⁻³	Porosity
Mid-Atlantic Ridge, cohesive carbonate clay:						
8	-39.999	-9.666	3409	0-2	1.27	0.68
				2-4	1.33	0.60
				4-6	1.38	0.67
				6-8	1.46	0.64
				8-10	1.46	0.64
Argentine Basin, cohesive red clay:						
18	-40.001	-42.416	5156	0-2	0.92	0.83
				2-4	1.02	0.79
				4-6	1.08	0.76
				6-8	1.16	0.74
				8-10	1.19	0.72
				10-12	1.21	0.72
Continental rise, cohesive hemipelagic clay:						
21	-37.026	-52.503	3323	0-2	1.16	0.66
				2-4	1.30	0.72
				4-6	1.42	0.66
				6-8	1.47	0.62
				8-10	1.42	0.65
Mid-slope Uruguayan margin, cohesive silty mud:						
22	-36.538	-53.102	1483	0-2	0.88	0.83
				2-4	0.98	0.79
				4-6	1.04	0.78
				6-8	1.06	0.76
				8-10	1.05	0.78
				10-12	1.06	0.75
Upper-slope Uruguayan margin, cohesive muddy silt:						
23	-36.338	-53.337	705	0-2	1.24	0.70
				2-4	1.47	0.62
				4-6	1.51	0.59
				6-8	1.64	0.56
				8-10	1.60	0.57
				10-12	1.57	0.58
Uruguayan shelf top, non-cohesive permeable sand:						
24	-36.000	-54.000	60	0-2	2.14	0.38
				2-4	2.14	0.40
				4-6	2.12	0.41
				6-8	2.04	0.36
				8-10	2.07	0.41

DBD   Dry Bulk Density; dry mass salt correction assumes 3.5 weight % of water content

Table S2. GA10W Sediment composition

Station	Water depth	Sed. depth	Opal dwt		CaCO$_3$[a] dwt		TOC[a] dwt		Lithogenic dwt	
	m	cm	%	2SE	%	2σ	%	2σ	%	2σ
8	3409	0.5	1.2	0.2	81.3	0.89	0.11	0.15	17.4	1.23
8	3409	1.5	0.9	0.1	82.7	0.89	0.15	0.15	16.3	1.13
8	3409	2.5	0.9	0.1	82.2	0.89	0.16	0.15	16.7	1.12
8	3409	3.5	0.5	0.1	82.0	0.89	0.23	0.15	17.3	1.12
8	3409	4.5	0.8	0.1	82.5	0.89	0.10	0.15	16.6	1.13
8	3409	6	0.7	0.1	81.0	0.89	0.25	0.15	18.0	1.12
8	3409	8	0.8	0.1	81.0	0.89	0.06	0.15	18.1	1.12
8	3409	10	0.9	0.1	79.8	0.89	0.01	0.15	19.2	1.12
8	3409	12	0.8	0.1	77.3	0.89	0.07	0.15	21.9	1.12
8	3409	14	1.0	0.1	75.8	0.89	0.13	0.15	23.1	1.13
8	3409	16	0.9	0.1	-	-	-	-	-	-
8	3409	18	0.9	0.1	71.0	0.89	0.03	0.15	28.1	1.13
8	3409	20	0.8	0.1	-	-	-	-	-	-
8	3409	22	0.9	0.1	69.5	0.89	-0.09	0.15	29.7	1.12
18	5156	0.5	13.5	0.7	0.26	0.23	0.97	0.25	85.3	1.23
18	5156	1.5	14.1	0.7	0.08	0.03	0.85	0.23	84.9	1.00
18	5156	2.5	14.7	0.8	0.09	0.13	0.81	0.24	84.4	1.19
18	5156	3.5	14.0	0.8	0.05	0.13	0.80	0.24	85.1	1.14
18	5156	4.5	15.1	0.9	0.02	0.13	0.82	0.24	84.1	1.23
18	5156	7	14.6	0.8	0.01	0.13	0.82	0.24	84.6	1.14
18	5156	11	12.3	0.7	0.02	0.13	0.59	0.24	87.0	1.02
18	5156	15	6.5	0.4	BDL	0.13	0.38	0.24	93.1	0.79
18	5156	19	5.5	0.3	BDL	0.13	0.31	0.24	94.1	0.72
18	5156	23	5.1	0.3	BDL	0.13	0.37	0.24	94.5	0.69
18	5156	27	4.3	0.3	0.00	0.13	0.67	0.24	95.1	0.64
18	5156	31	4.6	0.3	-	-	-	-	-	-
18	5156	35	5.5	0.3	-	-	-	-	-	-
21	3323	0.5	4.7	0.3	1.10	0.13	1.18	0.09	93.0	0.54
21	3323	1.5	4.7	0.3	0.20	0.13	1.24	0.09	93.8	0.53
21	3323	2.5	4.1	0.3	0.18	0.13	1.03	0.09	94.7	0.49
21	3323	3.5	4.6	0.3	0.20	0.13	1.24	0.09	94.0	0.52
21	3323	4.5	4.1	0.3	0.23	0.13	1.24	0.09	94.4	0.50
21	3323	5.5	4.4	0.3	0.25	0.13	1.03	0.09	94.3	0.53

21	3323	6.5	4.0	0.3	0.33	0.13	0.89	0.09	94.8	0.49
21	3323	7.5	2.8	0.2	0.49	0.13	0.84	0.09	95.9	0.45
21	3323	8.5	4.0	0.3	0.43	0.13	0.77	0.09	94.8	0.49
21	3323	9.5	4.0	0.3	0.26	0.13	0.71	0.09	95.0	0.49
22	1483	0.5	4.4	0.3	7.27	1.42	4.21	0.25	84.1	1.98
22	1483	1.5	3.5	0.2	8.48	1.42	3.97	0.25	84.1	1.87
22	1483	2.5	2.6	0.2	8.52	1.42	3.66	0.25	85.2	1.84
22	1483	3.5	3.2	0.2	8.61	1.42	3.92	0.25	84.3	1.87
22	1483	4.5	3.4	0.2	8.68	1.42	3.68	0.25	84.3	1.87
22	1483	5.5	4.1	0.2	8.61	1.42	3.75	0.25	83.5	1.89
22	1483	7	2.9	0.2	7.90	1.42	3.50	0.25	85.7	1.86
22	1483	9	3.3	0.2	-	-	-	-	-	-
22	1483	11	3.5	0.2	9.35	1.42	3.90	0.25	83.2	1.87
22	1483	13	2.8	0.2	-	-	-	-	-	-
22	1483	15	2.8	0.2	9.33	1.42	3.34	0.25	84.5	1.85
22	1483	17	3.3	0.2	-	-	-	-	-	-
22	1483	19	3.0	0.2	8.50	1.42	3.41	0.25	85.1	1.86
22	1483	21	2.8	0.2	-	-	-	-	-	-
22	1483	23	2.8	0.2	9.50	1.42	3.46	0.25	84.2	1.85
22	1483	25	3.1	0.2	-	-	-	-	-	-
22	1483	27	3.9	0.2	10.04	1.42	3.45	0.25	82.6	1.89
22	1483	29	3.3	0.2	-	-	-	-	-	-
23	705	0.5	1.7	0.2	2.09	0.18	1.68	0.10	94.5	0.47
23	705	1.5	1.6	0.1	1.91	0.04	2.08	0.08	94.4	0.23
23	705	2.5	2.1	0.1	1.80	0.17	1.47	0.10	94.6	0.40
23	705	3.5	1.4	0.1	1.87	0.24	1.51	0.11	95.3	0.45
23	705	4.5	1.3	0.1	1.88	0.26	1.50	0.11	95.3	0.47
23	705	5.5	1.0	0.1	2.36	0.18	1.57	0.10	95.0	0.37
23	705	7	0.9	0.1	2.67	0.18	1.56	0.10	94.9	0.36
23	705	9	1.2	0.1	3.01	0.18	1.26	0.10	94.5	0.38
23	705	11	1.2	0.1	-	-	-	-	-	-
23	705	13	1.1	0.1	3.49	0.18	1.42	0.10	94.0	0.37
23	705	15	1.0	0.1	-	-	-	-	-	-
23	705	17	0.8	0.1	3.92	0.18	1.56	0.10	93.8	0.36
23	705	19	1.5	0.1	-	-	-	-	-	-
23	705	21	1.2	0.1	4.33	0.18	1.75	0.10	92.8	0.37
23	705	23	1.3	0.1	-	-	-	-	-	-
23	705	25	1.0	0.1	4.85	0.18	1.98	0.10	92.2	0.37

23	705	27	1.1	0.1	-	-	-	-	-	-
23	705	29	0.9	0.1	3.23	0.18	1.65	0.10	94.2	0.37
24	60	0.5	0.3	0.2	-0.02	0.03	0.39	0.02	99.3	0.24
24	60	1.5	BDL	0.2	0.01	0.03	0.11	0.02	99.9	0.24
24	60	2.5	BDL	0.1	-0.08	0.03	0.13	0.02	100.0	0.19
24	60	3.5	0.1	0.1	0.12	0.03	0.11	0.02	99.7	0.20
24	60	4.5	0.0	0.1	0.09	0.03	0.13	0.02	99.8	0.12
24	60	5.5	0.2	0.1	0.01	0.03	0.23	0.02	99.5	0.12
24	60	7	BDL	0.1	0.12	0.03	0.17	0.02	99.7	0.12
24	60	9	BDL	0.1	0.12	0.03	0.48	0.02	99.4	0.12
24	60	11	BDL	0.1	0.68	0.03	0.18	0.02	99.1	0.12
24	60	13	0.1	0.1	0.53	0.03	0.18	0.02	99.1	0.12
24	60	15	0.3	0.1	2.10	0.03	0.01	0.02	97.6	0.12
24	60	17	0.2	0.1	2.89	0.03	0.18	0.02	96.8	0.12
24	60	19	0.5	0.1	2.03	0.03	0.38	0.02	97.1	0.12

\-   Not determined

BDL   Below detection limit

(a)   Station 8 $CaCO_3$ and TOC data previously reported by Bridgestock *et al.* (*13*)

Table S3. Summary of O₂ penetration, calculated flux[a] and C oxidation rate[b]

Station	Water depth m	O₂ penetration cm	O₂ flux mmol · m⁻² · d⁻¹	C_{ox} mmol · m⁻² · d⁻¹
8	3409	>8	0.84	0.64
18	5156	>9	0.42	0.32
21	3323	3.150	2.11	1.62
22	1483	0.725	8.35	6.41
23	705	0.400	23.40	17.97
24	60	1.625	-	-

\- Not determined

BDL Below detection limit

(a, b) Following the approach of Klar *et al.* (*11*)

Table S4. GA10W Porewater nutrient concentrations

Station	Water depth	Sed. depth	NO_2^-	NO_3^- + NO_2^- [a]	NH_4	$SiO4$
	m	cm	µmol l^{-1}	µmol l^{-1}	µmol l^{-1}	µmol l^{-1}
8	3409	0.5	2.76	40.59	33.06	126.11
8	3409	1.5	1.68	42.88	30.52	153.58
8	3409	2.5	0.81	44.80	45.36	173.95
8	3409	3.5	0.95	47.02	47.15	187.49
8	3409	4.5	0.69	50.88	47.02	201.36
8	3409	6.5	0.28	54.23	53.81	217.14
8	3409	8.5	0.06	45.65	73.95	217.07
8	3409	10.5	0.02	44.08	40.77	239.24
8	3409	12.5	0.01	44.00	29.75	246.33
8	3409	15.5	0.21	40.78	17.89	244.86
8	3409	18.5	0.11	47.93	105.57	262.84
8	3409	21.5	0.06	36.84	28.46	278.24
18	5156	0.5	1.44	39.61	20.55	167.70
18	5156	2.5	0.72	38.01	11.83	170.88
18	5156	4.5	0.51	39.59	9.92	211.95
18	5156	6.5	0.34	35.92	12.10	276.77
18	5156	9.5	0.22	32.90	9.68	296.92
18	5156	12.5	0.16	29.22	57.93	311.79
18	5156	15.5	0.16	21.44	43.83	323.76
18	5156	18.5	0.11	15.54	33.79	331.15
18	5156	22.5	0.13	8.46	36.70	338.94
18	5156	26.5	0.10	1.95	30.85	349.38
18	5156	30.5	0.12	1.61	34.40	356.80
21	3323	1	1.31	37.81	23.06	172.64
21	3323	2	2.52	31.80	24.21	200.52
21	3323	3	5.37	22.29	16.42	218.20
21	3323	4	4.51	10.67	-	242.17
21	3323	5	0.68	4.32	49.13	255.12
21	3323	6	0.95	2.19	31.85	256.15
21	3323	7	0.19	1.31	47.11	276.00
21	3323	8	0.13	1.16	57.23	281.75
21	3323	9	0.13	1.58	62.69	304.87
21	3323	10	0.15	1.96	71.01	305.89
22	1483	0.5	0.79	14.39	2.55	119.49

22	1483	2.5	0.55	2.77	21.82	211.13
22	1483	3.5	0.62	2.16	30.02	122.67
22	1483	4.5	0.42	1.56	36.71	219.14
22	1483	6.5	0.64	2.87	52.11	239.97
22	1483	8.5	0.37	1.86	52.59	223.49
22	1483	11.5	0.41	1.40	63.29	166.58
22	1483	14.5	0.39	1.70	73.76	291.91
22	1483	17.5	0.54	1.50	85.27	183.89
22	1483	20.5	0.47	1.15	89.73	120.14
22	1483	24.5	0.66	1.38	104.23	106.06
22	1483	28.5	0.42	0.99	119.79	314.27
23	705	0.5	1.06	4.43	8.86	78.96
23	705	1.5	1.05	2.26	16.71	126.29
23	705	2.5	0.80	2.47	35.32	135.81
23	705	3.5	0.90	1.61	38.12	159.84
23	705	4.5	1.83	2.15	46.96	210.55
23	705	6.5	2.12	2.22	61.05	273.13
23	705	8.5	1.98	1.87	68.54	203.77
23	705	11.5	1.74	1.78	62.91	196.76
23	705	14.5	0.77	0.83	59.75	171.82
23	705	17.5	1.29	1.21	63.82	109.91
23	705	20.5	1.24	1.33	76.44	106.75
23	705	24.5	0.84	0.91	82.23	131.37
24	60	0.5	1.29	21.22	4.20	75.34
24	60	1.5	0.86	17.12	10.96	78.86
24	60	3.5	1.02	5.72	36.29	63.85
24	60	4.5	1.13	4.73	36.01	52.35
24	60	5.5	0.60	2.29	35.00	55.05
24	60	7.5	0.52	2.15	32.97	44.74
24	60	8.5	0.86	2.00	29.94	34.95
24	60	10.5	0.79	1.55	25.81	32.44
24	60	12.5	0.57	1.13	27.03	32.09

(a) NO_3^- + NO_2^- data previously reported for by Bridgestock et al. (13)

Table S5. GA10W Porewater Mn, Fe and Fe isotope compositions

Stn.	Sed. depth cm	dMn µmol l⁻¹	2σ	sMn µmol l⁻¹	2σ	dFe[a] µmol l⁻¹	2σ	sFe µmol l⁻¹	2σ	δ⁵⁶dFe ‰	2σ
8	0.5	0.111	0.003	0.112	0.003	0.025	0.000	0.025	0.000	-	
8	1.5	0.090	0.002	-		0.054	0.001	-		-	
8	2.5	0.081	0.002	-		0.050	0.001	-		-	
8	3.5	0.082	0.002	-		0.005	0.000	-		-	
8	4.5	0.075	0.002	-		0.011	0.000	-		-	
8	6	0.074	0.002	0.074	0.002	0.013	0.000	BDL		-	
8	8	0.068	0.002	-		0.019	0.000	-		-	
8	10	0.069	0.002	-		0.040	0.001	-		-	
8	12	0.070	0.002	-		0.036	0.001	-		-	
8	14	0.073	0.002	-		0.112	0.002	-		-	
8	16	0.067	0.002	-		0.013	0.000	-		-	
8	18	0.067	0.002	-		0.005	0.000	-		-	
8	20	0.070	0.002	-		0.022	0.000	-		-	
8	22	0.072	0.002	0.070	0.002	0.059	0.001	0.022	0.000	-	
18	0.5	0.028	0.001	0.022	0.001	0.064	0.001	0.024	0.000	-	
18	1.5	0.008	0.000	-		0.030	0.001	-		-	
18	2.5	0.007	0.000	0.005	0.000	0.049	0.001	BDL		-	
18	3.5	0.007	0.000	-		0.038	0.001	-		-	
18	4.5	0.008	0.000	0.007	0.000	0.097	0.002	0.009	0.000	-	
18	5.5	0.004	0.000	-		0.056	0.001	-		-	
18	7	0.008	0.000	0.003	0.000	0.237	0.005	BDL		0.11	0.06
18	9	0.005	0.000	-		0.175	0.004	-		-	
18	11	0.010	0.000	-		0.115	0.002	-		-	
18	13	0.085	0.002	0.084	0.002	0.164	0.003	BDL		-	
18	15	0.477	0.012	-		0.036	0.001	-		-	
18	17	1.465	0.038	-		0.056	0.001	-		-	
18	19	3.310	0.086	3.40	0.088	0.127	0.003	0.009	0.000	-	
18	21	3.713	0.097	-		0.085	0.002	-		-	
18	23	3.493	0.091	3.54	0.092	0.130	0.003	0.012	0.000	-	
18	25	2.344	0.061	-		0.109	0.002	-		-	
18	27	7.675	0.200	7.79	0.203	0.216	0.004	0.022	0.000	0.11	0.06
18	29	7.233	0.188	-		0.953	0.019	-		-0.91	0.03
18	31	10.09	0.262	10.5	0.274	1.069	0.021	0.89	0.018	-0.91	0.02
18	33	10.41	0.271	-		1.830	0.037	-		-0.89	0.03
18	35	7.111	0.185	-		6.568	0.131	-		-0.81	0.03
21	0.5	0.095	0.002	0.088	0.002	0.179	0.004	0.012	0.000	0.03	0.07
21	1.5	0.026	0.001	0.019	0.000	0.251	0.005	0.004	0.000	0.04	0.06

21	2.5	0.031	0.001	0.021	0.001	0.353	0.007	0.005	0.000	0.05	0.06
21	3.5	0.019	0.000	0.008	0.000	0.514	0.010	0.006	0.000	0.14	0.05
21	4.5	0.013	0.000	0.011	0.000	0.311	0.006	0.014	0.000	0.08	0.05
21	5.5	0.201	0.005	-		0.265	0.005	-		0.16	0.06
21	6.5	0.365	0.010	0.360	0.009	0.514	0.010	0.087	0.002	-0.01	0.04
21	7.5	0.531	0.014			0.755	0.015	-		-0.80	0.03
21	8.5	0.638	0.017	0.637	0.017	1.520	0.030	0.892	0.018	-0.82	0.03
21	9.5	3.268	0.085	-		0.634	0.013	-		-0.44	0.05
22	0.5	0.073	0.002	0.069	0.002	0.237	0.005	0.032	0.001	-0.06	0.06
22	1.5	1.312	0.034	-		1.498	0.030	-		-0.24	0.03
22	2.5	1.663	0.043	1.62	0.042	11.19	0.224	10.6	0.213	-1.77	0.03
22	3.5	1.733	0.045	-		15.46	0.309	-		-1.23	0.03
22	4.5	1.619	0.042	1.63	0.042	19.32	0.386	18.8	0.376	-1.24	0.03
22	5.5	1.647	0.043	-		22.31	0.446	-		-1.27	0.04
22	7	1.852	0.048	1.84	0.048	52.43	1.049	51.1	1.022	-1.30	0.03
22	9	2.144	0.056	-		52.25	1.045	-		-0.47	0.03
22	11	2.367	0.062	2.33	0.061	52.27	1.045	50.6	1.012	-	
22	13	2.773	0.072	-		48.61	0.972	-		-0.50	0.03
22	15	2.813	0.073	2.81	0.073	31.78	0.636	30.4	0.608	-	
22	17	2.710	0.070	-		23.31	0.466	-		-0.27	0.03
22	19	2.763	0.072	2.76	0.072	16.97	0.339	15.8	0.316	-	
22	21	2.560	0.067	-		8.757	0.175	-		0.26	0.02
22	23	2.359	0.061	-		2.938	0.059	-		-	
22	25	2.104	0.055	-		1.544	0.031	-		0.63	0.03
22	27	1.888	0.049	-		0.895	0.018	-		-	
22	29	1.686	0.044	-		0.769	0.015	-		0.63	0.05
23	0.5	1.713	0.045	-		2.457	0.049	-		-1.37	0.03
23	1.5	1.581	0.041	-		19.47	0.389	-		-0.78	0.03
23	2.5	1.371	0.036	-		13.42	0.268	-		-0.77	0.03
23	3.5	1.147	0.030	-		10.90	0.218	-		-1.15	0.03
23	4.5	1.368	0.036	-		13.67	0.273	-		-1.13	0.04
23	5.5	1.104	0.029	-		5.078	0.102	-		-0.89	0.05
23	7	1.016	0.026	-		3.792	0.076	-		0.05	0.04
23	9	0.997	0.026	-		1.956	0.039	-		-	
23	11	0.834	0.022	-		0.697	0.014	-		0.32	0.04
23	13	0.653	0.017	-		0.391	0.008	-		-	
23	15	0.652	0.017	-		0.687	0.014	-		-	
23	17	0.617	0.016	-		0.418	0.008	-		0.34	0.05
23	19	0.641	0.017	-		0.348	0.007	-		-	
23	21	0.660	0.017	-		0.460	0.009	-		-	
23	23	0.669	0.017	-		0.530	0.011	-		0.39	0.05

23	25	0.684	0.018	-	0.349	0.007	-	-	
23	27	0.685	0.018	-	0.404	0.008	-	-	
23	29	0.673	0.018	-	0.297	0.006	-	0.37	0.05
24	0.5	0.719	0.019	-	0.314	0.006	-	0.15	0.10
24	1.5	0.568	0.015	-	0.040	0.001	-	-	
24	2.5	0.838	0.022	-	0.529	0.011	-	-	
24	3.5	1.008	0.026	-	22.17	0.443	-	-0.93	0.03
24	4.5	0.441	0.011	-	6.703	0.134	-	-0.88	0.04
24	5.5	0.433	0.011	-	3.888	0.078	-	-0.30	0.03
24	6.5	0.330	0.009	-	2.511	0.050	-	-0.15	0.05
24	7.5	0.346	0.009	-	1.995	0.040	-	-0.34	0.03
24	8.5	0.289	0.008	-	1.046	0.021	-	-	
24	10.5	0.291	0.008	-	1.016	0.020	-	-0.32	0.03
24	12.5	0.296	0.008	-	0.608	0.012	-	0.10	0.04
24	14.5	0.510	0.013	-	0.105	0.002	-	-	
24	17.5	0.887	0.023	-	0.061	0.001	-	-	

-      Not determined

BDL   Below detection limit

(a)   dFe data previously reported by Bridgestock *et al.* (*13*)

Table S6. Summary of inputs to porewater REC model

Depth cm	Fe[(a)] μM	Porosity[(b)]	Bioturbation $cm^2 \cdot s^{-1}$	Sedimentation $cm \cdot s^{-1}$	Irrigation s^{-1}	Diffusion[(c)] $cm^2 \cdot s^{-1}$
REC Model inputs for station 21 dissolved Fe						
-0.1	0.01	0.66	0	0	0	3.77548E-06
0.5	0.179	0.66	0	0	0	3.77548E-06
1.5	0.251	0.66	0	0	0	3.77548E-06
2.5	0.353	0.66	0	0	0	3.77548E-06
3.5	0.514	0.66	0	0	0	3.77548E-06
4.5	0.311	0.66	0	0	0	3.77548E-06
5.5	0.265	0.66	0	0	0	3.77548E-06
6.5	0.514	0.66	0	0	0	3.77548E-06
7.5	0.755	0.66	0	0	0	3.77548E-06
8.5	1.520	0.66	0	0	0	3.77548E-06
REC Model inputs for station 21 soluble Fe						
-0.1	0.001	0.66	0	0	0	3.77548E-06
0.5	0.012	0.66	0	0	0	3.77548E-06
1.5	0.004	0.66	0	0	0	3.77548E-06
2.5	0.005	0.66	0	0	0	3.77548E-06
3.5	0.006	0.66	0	0	0	3.77548E-06
4.5	0.014	0.66	0	0	0	3.77548E-06
6.5	0.087	0.66	0	0	0	3.77548E-06
8.5	0.892	0.66	0	0	0	3.77548E-06

(a) sFe and dFe derived from Table S5

(b) Mean value derived from Table S1

(c) Assumes ionic Fe^{2+} where T is 4.0°C, salinity is 34.75, P is 330atm

References

1.   W. B. Homoky, S. G. John, T. Conway, R. A. Mills, Distinct iron isotopic signatures and supply from marine sediment dissolution. *Nature Communications* **4**, (2013).
2.   B. L. Beard, C. M. Johnson, Fe Isotope Variations in the Modern and Ancient Earth and Other Planetary Bodies. *Reviews in Mineralogy and Geochemistry* **55**, 319-357 (2004).
3.   A. D. Anbar, Iron stable isotopes: beyond biosignatures. *Earth and Planetary Science Letters* **217**, 223-236 (2004).
4.   T. D. Bullen, A. F. White, C. W. Childs, D. V. Vivit, M. S. Schulz, Demonstration of significant abiotic iron isotope fractionation in nature. *Geology* **29**, 699-702 (2001).
5.   O. Rouxel, E. Sholkovitz, M. Charette, K. J. Edwards, Iron isotope fractionation in subterranean estuaries. *Geochimica et Cosmochimica Acta* **72**, 3413-3430 (2008).
6.   A. J. M. Lough *et al.*, Opposing authigenic controls on the isotopic signature of dissolved iron in hydrothermal plumes. *Geochimica et Cosmochimica Acta* **202**, 1-20 (2017).
7.   O. Rouxel, B. Toner, Y. Germain, B. Glazer, Geochemical and iron isotopic insights into hydrothermal iron oxyhydroxide deposit formation at Loihi Seamount. *Geochimica et Cosmochimica Acta* **220**, 449-482 (2018).
8.   S. G. John, J. Adkins, The verticle distribution of iron stable isotopes in the North Atlantic near Bermuda. *Global Biogeochem. Cycles* **26**, GB2034 (2012).
9.   M. Staubwasser, R. Schoenberg, F. von Blanckenburg, S. Krüger, C. Pohl, Isotope fractionation between dissolved and suspended particulate Fe in the oxic and anoxic water column of the Baltic Sea. *Biogeosciences* **10**, 233-245 (2013).
10.   S. Henkel, S. Kasten, S. W. Poulton, M. Staubwasser, Determination of the stable iron isotopic composition of sequentially leached iron phases in marine sediments. *Chemical Geology* **421**, 93-102 (2016).
11.   J. K. Klar *et al.*, Stability of dissolved and soluble Fe(II) in shelf sediment pore waters and release to an oxic water column. *Biogeochemistry*, 1-19 (2017).
12.   R. A. Berner, *Early Diagenesis: A Theoretical Approach*. H. D. Holland, Ed., Princeton Series in Geochemistry (Princeton University Press, Princeton, NJ, 1980), pp. 241.
13.   L. Bridgestock *et al.*, Controls on the barium isotope compositions of marine sediments. *Earth and Planetary Science Letters* **481**, 101-110 (2018).